

## BIROn - Birkbeck Institutional Research Online

Jordan, S.F. and Rammu, H. and Zheludev, I.N. and Hartley, Andrew and Marechal, Amandine and Lane, N. (2019) Promotion of protocell self-assembly from mixed amphiphiles at the origin of life. *Nature Ecology & Evolution* , ISSN 2397-334X.

Downloaded from: <http://eprints.bbk.ac.uk/29841/>

*Usage Guidelines:*

Please refer to usage guidelines at <http://eprints.bbk.ac.uk/policies.html> or alternatively contact [lib-eprints@bbk.ac.uk](mailto:lib-eprints@bbk.ac.uk).

1 **Promotion of protocell self-assembly from mixed amphiphiles at the origin of life**

2

3 Sean F. Jordan<sup>1</sup>, Hanadi Rammu<sup>1</sup>, Ivan N. Zheludev<sup>1</sup>, Andrew M. Hartley<sup>2</sup>, Amandine Maréchal<sup>2,3</sup>,

4 Nick Lane<sup>1</sup>

5

6 <sup>1</sup>*Centre for Life's Origin and Evolution, Department of Genetics, Evolution and Environment, Darwin*

7 *Building, Gower Street, University College London, London WC1E 6BT, UK*

8 <sup>2</sup>*Institute of Structural and Molecular Biology, Birkbeck College, London, WC1E 7HX, UK*

9 <sup>3</sup>*Institute of Structural and Molecular Biology, University College London, London, WC1E 6BT, UK*

10

11 **Corresponding author:** Nick Lane [nick.lane@ucl.ac.uk](mailto:nick.lane@ucl.ac.uk)

12

13 **Key words:** origin of life, protocells, single-chain amphiphiles, fatty acids, 1-alkanols, vesicles,

14 alkaline hydrothermal vents, self-assembly

15

16 **Abstract**

17

18 Vesicles formed from single-chain amphiphiles (SCAs) such as fatty acids likely played an important

19 role in the origin of life. A major criticism of the hypothesis that life arose in an early ocean

20 hydrothermal environment is that hot temperatures, large pH gradients, high salinity and abundant

21 divalent cations should preclude vesicle formation. But these arguments are based on model vesicles

22 using 1-3 SCAs, even though Fischer-Tropsch-type synthesis under hydrothermal conditions

23 produces a wide array of fatty acids and 1-alkanols, including abundant C<sub>10</sub>-C<sub>15</sub> compounds. Here we

24 show that mixtures of these C<sub>10</sub>-C<sub>15</sub> SCAs form vesicles in aqueous solutions between pH ~6.5 to >12

25 at modern seawater concentrations of NaCl, Mg<sup>2+</sup> and Ca<sup>2+</sup>. Adding C<sub>10</sub> isoprenoids improves vesicle

26 stability even further. Vesicles form most readily at temperatures of ~70 °C and require salinity and

27 strongly alkaline conditions to self-assemble. Thus, alkaline hydrothermal conditions not only permit  
28 protocell formation at the origin of life but actively favour it.

29

### 30 **Introduction**

31

32 Membranes are fundamental to life, the nexus between cell and environment. Peter Mitchell wrote  
33 “I cannot consider the organism without its environment... from a formal point of view the two may  
34 be regarded as equivalent phases between which dynamic contact is maintained by the membranes  
35 that separate and link them”<sup>1</sup>. Beyond the requirement for compartmentalisation, differences in ion  
36 concentration across the plasma membrane drive CO<sub>2</sub> fixation and energy metabolism in all modern  
37 autotrophic cells by vectorial chemistry<sup>2-4</sup>. This deep conservation of membrane bioenergetics also  
38 points to the fundamental role of membranes at the origin of life<sup>2-4</sup>.

39

          Despite their clear importance across life, the composition of early membranes is uncertain.  
40 The universality of membrane proteins with equivalent transmembrane helices indicates that early  
41 cells had some sort of lipid bilayer<sup>5</sup>. But the phospholipid membranes of bacteria and archaea differ  
42 in their chemistry, most strikingly in the stereochemistry of their glycerol phosphate headgroups –  
43 archaea typically have glycerol-1-phosphate while bacteria have glycerol-3-phosphate<sup>6-8</sup>. There is no  
44 known selective basis for this distinction<sup>9</sup>, suggesting that their common ancestor did not possess a  
45 modern phospholipid membrane but instead had a simpler bilayer composed largely of single-chain  
46 amphiphiles (SCAs), perhaps including fatty acids and isoprenoids (which are found in both bacteria  
47 and archaea<sup>10</sup>, and are perfectly compatible membrane components<sup>11,12</sup>). SCAs can assemble to  
48 form droplets, micelles or lipid bilayers in aqueous solutions depending on pH (Extended Data Fig.  
49 1). Bilayer membranes composed of SCAs facilitate simple growth, being able to incorporate new  
50 lipids directly<sup>13-15</sup>. In principle, proton-permeable SCA membranes are also required for cells to  
51 harness geological ion gradients without collapsing to equilibrium, potentially shedding light on the  
52 deep divergence between bacteria and archaea<sup>4,16</sup>.

53           The idea that the first cell membranes were composed of SCAs is appealing from the  
54 standpoint of prebiotic chemistry<sup>17,18</sup>. Fatty-acid synthesis is thermodynamically favoured under mild  
55 hydrothermal conditions (25-150 °C) at alkaline pH<sup>19</sup>. Lipids have been synthesised from formate via  
56 Fischer-Tropsch-type reactions under hydrothermal conditions (100-150 °C), albeit in steel reactors,  
57 suggesting that iron (or carbon-metal bonds<sup>20</sup>) might be a critical electron donor or catalyst<sup>21</sup>. The  
58 lipids formed include abundant long-chain fatty acids and 1-alkanols (mainly C<sub>6</sub>-C<sub>16</sub>)<sup>21</sup>. Likewise, the  
59 reaction of acetylene (C<sub>2</sub>H<sub>2</sub>) and CO in contact with nickel sulfide (NiS) in hot aqueous medium at pH  
60 7-9 can form long-chain (up to C<sub>9</sub>) unsaturated monocarboxylic acids<sup>22</sup>. Branched-chain pentoses  
61 containing the isoprene skeleton are formed under mild alkaline hydrothermal conditions (60-90 °C,  
62 pH 9-11) via the formose reaction<sup>23</sup>. Higher pressure in submarine hydrothermal vents should favour  
63 synthesis of longer-chain amphiphiles, according to Le Chatelier's principle<sup>21</sup>, as well as greatly  
64 increasing hydrogen solubility<sup>24</sup>. Thermophoresis in porous hydrothermal systems can concentrate  
65 amphiphiles above the critical bilayer concentration to form vesicles spontaneously<sup>25,26</sup>. Mineral  
66 surfaces including silicates and FeS minerals found in hydrothermal systems can also enhance vesicle  
67 assembly<sup>27</sup>. Theoretical modelling suggests that vectorial CO<sub>2</sub> reduction on FeS clusters associated  
68 with protocell membranes (which are homologous to the proton-motive Energy-converting  
69 hydrogenase in methanogens<sup>28</sup>) could drive protocellular growth and establish a rudimentary form  
70 of membrane heredity<sup>29</sup>. All these factors point to alkaline hydrothermal systems as prebiotic  
71 electrochemical reactors<sup>4,7,30-35</sup> capable of driving the synthesis of amphiphiles, and then  
72 concentrating them *in situ*, to form protocells at the origin of life.

73           But there is also a potentially serious drawback. One of the major criticisms of alkaline  
74 hydrothermal vents as a setting for the origin of life is that the relatively harsh environment is not  
75 conducive to the formation of vesicles<sup>36-39</sup>. Specifically, previous laboratory work has shown that  
76 strongly alkaline pH, high temperatures, ocean salinity and abundant divalent cations all disrupt the  
77 formation of vesicles from SCAs<sup>36-40</sup>. The conclusion that amphiphilic compounds 'do not assemble  
78 into vesicles in seawater' might seem fatal to the idea that life originated in deep-sea hydrothermal

79 vents<sup>40</sup>. Yet this conclusion is based on vesicles composed of decanoic acid or simple mixtures of two  
80 or three amphiphiles. Mixtures of SCAs with more complex head groups (such as amine, glycerol,  
81 and sulfate) have been shown to form vesicles over a wider pH range, albeit predominantly at  
82 neutral and acidic pH<sup>41,42</sup>. The addition of 1-alkanols can stabilize fatty-acid vesicles at the high pH  
83 found in alkaline vents<sup>43,44</sup>. Vesicles composed of decylamine and decanoic acid are stable even at  
84 pH 11 in the presence of some salts, but they produce curious crystalline aggregates between pH 2  
85 and 10, while their prebiotic provenance is uncertain<sup>45</sup>. Polyaromatic hydrocarbons (PAH) seem to  
86 improve vesicle stability further, although they have little congruence with modern membranes<sup>45,46</sup>.  
87 Yet despite these various indications that mixtures of amphiphiles can enhance vesicle stability, the  
88 combination of strongly alkaline pH, high temperatures, high salinity and abundant divalent cations  
89 is still often cited as an insuperable barrier to life beginning in oceanic hydrothermal systems<sup>36-40</sup>.  
90 We have therefore explored the properties of vesicles assembled from mixtures of the 6-12 most  
91 abundant SCAs formed through hydrothermal Fischer-Tropsch-type synthesis<sup>21</sup>, combined with two  
92 simple isoprenoid molecules. Far from precluding vesicle formation at the origin of life, we show  
93 that alkaline hydrothermal conditions in fact promote vesicle assembly from these prebiotically  
94 plausible mixtures of amphiphiles.

95

## 96 **Results**

97 A 50 mM solution of pure decanoic acid vesicles (one of the most widely investigated vesicle forming  
98 SCAs in origin of life research) was first tested to ensure that the methods employed here yielded  
99 results matching literature values. These results provided a transition point of pH ~7.2 and a range of  
100 vesicle formation of ~0.2 pH units, which is similar to previously reported values (Fig. 1)<sup>47</sup>. The first  
101 complex solution of vesicles that we investigated was a mixture of fatty acids from C<sub>10</sub> to C<sub>15</sub>  
102 including both odd and even chain-lengths (all of which are formed by Fischer-Tropsch-type  
103 synthesis under hydrothermal conditions) giving a total of six SCAs. A concentration of 5 mM (of  
104 each SCA) was used to test vesicle stability across a pH range of ~7 to 13. When fitted to a sigmoid

105 curve (see Supplementary Information) a transition point of pH  $\sim$ 8.45 was observed (Fig. 1). Confocal  
106 microscopy of the solution at this pH value confirmed the presence of vesicles (Fig. 1). A greater  
107 abundance of vesicles was observed at pH values below these transition points (Supplementary Figs.  
108 1 and 2). The transition point appears to be a conservative estimate of the initiation point of vesicle  
109 formation, as confocal microscopy shows the presence of vesicles in mixed fatty acid solutions as  
110 high as pH  $\sim$ 9 whereas the observed transition point is pH  $\sim$ 8.5 (Supplementary Fig. 3).

111 Solutions containing fatty acids and 1-alkanols were prepared in molar ratios of 10:1, 5:1,  
112 and 1:1. The pH range of vesicle formation was unaffected by the addition of 1-alkanols in a 10:1  
113 ratio, giving a transition point of pH  $\sim$ 8.5, similar to that of fatty acids alone (Extended Data Fig. 2).  
114 But with a 5:1 ratio, the range was extended to a transition point of pH  $\sim$ 9.5 (Fig. 1). For a solution  
115 containing a 1:1 ratio of fatty acids to 1-alkanols vesicle formation was observed from pH  $\sim$ 6.5 to 13  
116 with no obvious transition point (Fig. 2a). Confocal microscopy confirms the presence of vesicles in  
117 solution across the entire pH range (Fig. 2). Encapsulation of the fluorescent dye pyranine clearly  
118 shows that these vesicles can trap and retain the dye (Fig. 3a) for periods of at least 24 h at pH 12  
119 (Fig. 3b) confirming that they have an aqueous lumen and are stable over hours to days. Note that  
120 the fluorescence associated with vesicles after 24 h had fallen to 15-20% that of fresh vesicles.

121 The CBC of the mixed fatty acid solution was determined to be 1.3 mM by OD  
122 measurements (Fig. 4), with each SCA at a concentration of 225  $\mu$ M. However, confocal microscopy  
123 at concentrations below 6 mM (combined SCA) did not reveal any vesicles in these solutions. We  
124 hypothesised that at lower concentrations, vesicles are smaller in size than those at higher  
125 concentrations. To test this, cryo-TEM analysis was conducted on mixed fatty acid solutions below 6  
126 mM concentration (with individual SCA concentrations of 100, 200, 300, 400, and 500  $\mu$ M). These  
127 results showed that vesicles did in fact form in solutions as low as 600  $\mu$ M total concentration but  
128 they were less than 200 nm in diameter, lower than the resolution limit of the confocal microscope  
129 (Fig. 4). These tiny vesicles do appear to have bounding membranes on cryo-TEM, although their  
130 appearance is equivocal, and it is possible that they are lipid droplets. Nonetheless, NS-TEM shows

131 unequivocal evidence of the collapsed doughnut shapes associated with vesicles, on an equivalent  
132 scale (Extended Data Figs. 3 and 4). We therefore think it most likely that low concentrations of SCAs  
133 do simply produce smaller vesicles. These small vesicles were present in higher concentration  
134 solutions as well and are likely present at most concentrations tested but are simply not observable  
135 under a confocal microscope. If so, then the CBC determined by the OD analysis is a conservative  
136 estimate of the minimum SCA concentration required for vesicle formation, as OD measurements  
137 are diffraction-limited in the same way as confocal microscopy. CBC values for the 5:1 and 1:1  
138 solutions were similar to those of fatty acids alone, and vesicles likely form below this concentration  
139 in these solutions as well (Extended Data Fig. 5).

140           Due to the extremely wide pH range of vesicle formation observed for 5 mM 1:1 solutions,  
141 this model was selected for further testing under the influence of salinity and divalent cations.  
142 Solutions were prepared in a range of conditions and analysed by confocal microscopy, cryo-TEM,  
143 NS-TEM and pyranine encapsulation. Modern day seawater contains on average 600 mM NaCl, 50  
144 mM Mg<sup>2+</sup>, and 10 mM Ca<sup>2+</sup>. These values are frequently cited as precluding the assembly of SCA  
145 vesicles, excluding any oceanic environment as a potential location for the origin of life<sup>39,40</sup>. As such,  
146 these concentrations were employed as the maximum concentrations for our experiments on the  
147 effects of salinity and divalent cations on vesicle formation, up to an ionic strength in the full salt mix  
148 of 1.022 M (Supplementary Table 1). Vesicles were prepared in a range of 100 – 600 mM NaCl at pH  
149 ~9 and 12 and were observed in all solutions at pH ~12 (Fig. 5, Extended Data Fig. 6 and  
150 Supplementary Fig. 4). Vesicles were prepared from 10 – 50 mM MgCl<sub>2</sub> and 1 – 10 mM CaCl<sub>2</sub> at pH  
151 ~7, 9, and 12. Again, vesicle formation was observed at all concentrations at pH ~12 (Fig. 5, Extended  
152 Data Figs. 7 and 8 and Supplementary Figs. 5 and 6) but no vesicles were observed at pH 7 or 9 in the  
153 presence of 20 mM MgCl<sub>2</sub> or 5 mM CaCl<sub>2</sub> (Supplementary Fig. 7), so we did not test higher  
154 concentrations. Vesicles were formed at lower concentrations of salt and divalent cations below pH  
155 12. Vesicles could also form long filaments, seen by both confocal microscopy and NS-TEM. While  
156 their structure was unclear by confocal microscopy, the filaments appeared to be composed of

157 chains of individual vesicles by NS-TEM (Fig. 6). Note that vesicles burst under vacuum and so appear  
158 collapsed during microscopy.

159 Finally, 5 mM 1:1 fatty acid:1-alkanol vesicles were prepared in an alkaline (pH >12) solution  
160 containing a combination of NaCl, Mg<sup>2+</sup>, and Ca<sup>2+</sup> at modern seawater concentrations, thereby  
161 providing a more realistic analogue environment. Under these conditions, individual vesicles were  
162 not formed, and aggregates of vesicles were the predominant structures seen. It should be noted  
163 that cooling of vesicle solutions has been shown to lead to aggregation<sup>40</sup>. As the microscope stage  
164 used here was not heated, cooling of the solutions from their original 70 °C temperature may also  
165 have contributed to this aggregation. This experiment was repeated with the addition of equimolar  
166 amounts of two C<sub>10</sub> isoprenoids, geranic acid and geraniol, which are prebiotically plausible  
167 molecules that are significantly under-researched in terms of their potential for prebiotic vesicle  
168 formation. The inclusion of these two compounds enabled the formation of vesicles in an alkaline  
169 solution (pH 12) containing a combination of 600 mM NaCl, 50 mM Mg<sup>2+</sup>, and 10 mM Ca<sup>2+</sup> observed  
170 by confocal microscopy and cryo-TEM (Fig. 7) and confirmed by NS-TEM (Extended Data Fig. 9 and  
171 Supplementary Figs. 8-10).

172 To demonstrate that the vesicles observed independently by several different types of  
173 microscopy are indeed stable vesicles with a lumen, we examined their encapsulation of pyranine.  
174 Fig. 3c shows that vesicles composed of the full amphiphile mix can encapsulate pyranine in water,  
175 while Fig. 3d shows that the dye is retained over at least 24 h, demonstrating the stability of these  
176 vesicles. However, encapsulation experiments are more problematic under high salt conditions,  
177 especially in the presence of divalent cations, as most dyes, including the standards normally used  
178 for vesicle work, pyranine and calcein, interact with divalent cations or precipitate as hydroxides<sup>48,49</sup>  
179 (Supplementary Fig. 11). Control preparations of pyranine in water with or without salts (i.e. with no  
180 SCAs present) show that pyranine fluorescence is largely suppressed in the presence of salts (Fig.  
181 3e). Despite these issues, by preparing vesicles in the presence of pyranine, and adding a double-  
182 concentration salt mixture to achieve the required total salt concentration after encapsulation, we



183 were able to demonstrate that 1:1:1 mixtures of all SCAs can indeed form stable vesicles capable of  
184 encapsulating the dye in alkaline solution (pH 12) containing a combination of 600 mM NaCl, 50 mM  
185  $Mg^{2+}$ , and 10 mM  $Ca^{2+}$  (Fig. 3f). We note these vesicles are able to retain the dye despite the osmotic  
186 shock of being added to double-strength full-salt mixtures. We also achieved encapsulation with  
187 calcein, despite interactions with salts (Extended Data Fig. 10). These findings confirm the cryo-TEM,  
188 confocal microscopy and NS-TEM demonstrating that vesicles are indeed formed under oceanic  
189 alkaline hydrothermal conditions.

190

## 191 **Discussion**

192 Our results show that mixtures of 6-14 SCAs, including fatty acids, 1-alkanols and isoprenoids, can  
193 form stable vesicles in aqueous solution across a pH range of ~6 units from pH ~6.5 to >12. We have  
194 demonstrated vesicle stability under these conditions by encapsulation of the fluorescent dye  
195 pyranine over 24 h (Fig. 3) and shown the presence of vesicles by multiple methodologically wholly  
196 distinct techniques, including cryo-TEM, NS-TEM, confocal microscopy, UV-Vis and fluorescence  
197 spectroscopy. Warm (70 °C), alkaline (pH 12) solutions equivalent to those found in modern alkaline  
198 hydrothermal vents<sup>34,50,51</sup> actively promote vesicle formation and mitigate the interference produced  
199 by high concentrations of NaCl,  $Mg^{2+}$ , and  $Ca^{2+}$ . In Hadean deep-ocean alkaline hydrothermal  
200 systems, vesicles should have formed readily from mixtures of prebiotic SCAs, likely produced by  
201 Fischer-Tropsch-type synthesis<sup>21</sup>, giving rise to protocells at the origin of life.

202 Hydrothermal Fischer-Tropsch-type synthesis has been shown to form complex mixtures of  
203 fatty acids and 1-alkanols, as well as long-chain alkanes and alkenes, which decrease in their  
204 abundance with chain lengths above ~15 carbons<sup>21</sup>. We therefore used mixtures of these SCAs with  
205 chain-lengths from  $C_{10}$ - $C_{15}$ . Compared with the  $C_{10}$  decanoic acid, longer chain lengths lower the  
206 critical bilayer concentration (CBC) by promoting more interactions between hydrophobic tails<sup>52,53</sup>,  
207 effectively decreasing fatty acid solubility. Mixtures of fatty acids and 1-alkanols decrease the CBC  
208 still further, presumably through hydrogen bonding between the carboxylate and alcohol

209 headgroups<sup>37,38,41,54</sup>. Vesicles assembled from decanoic acid alone have a CBC of 39 mM, whereas  
210 mixtures of 12 C<sub>10</sub>-C<sub>15</sub> fatty acids and 1-alkanols (1:1) have a CBC around 30-fold lower, at 1.3 mM  
211 with a concentration of 225 μM for each individual SCA. In fact, we found plentiful very small (<200  
212 nm diameter) vesicles by NS-TEM and cryo-TEM at even lower concentrations (100 μM for each SCA;  
213 Fig. 4). In vents, a combination of hydrothermal Fischer-Tropsch-type synthesis (producing complex  
214 mixtures of SCAs with low CBCs<sup>21</sup>) with thermophoresis (concentrating SCAs above the CBC via  
215 thermal currents<sup>25,26</sup>) and interactions with mineral surfaces (enhancing vesicle assembly<sup>27</sup>) should  
216 promote vesicle formation even at very low SCA concentrations.

217 More complex SCA mixtures dramatically increase vesicle assembly under strongly alkaline  
218 conditions. Raising the number of fatty acids in solution from one to six expands the pH range of  
219 vesicle formation nearly 100-fold, from about 0.2 to almost 2 pH units (Fig. 1). Increasing the content  
220 of 1-alkanols elicits an even greater effect. In 1:1 mixtures with fatty acids, 1-alkanols produce stable  
221 vesicles above pH 12, as seen from the OD data, confocal images (Fig. 2) and encapsulation of the  
222 fluorescent dye pyranine over 24 h (Fig. 3). Vesicles form when amphiphiles are in solution at a pH  
223 close to their pK<sub>a</sub>, meaning they exist in both their protonated and deprotonated forms<sup>55</sup>. Hydrogen  
224 bonding between protonated and deprotonated headgroups stabilizes bilayer structures. In  
225 contrast, protonation under acidic conditions promotes the formation of droplets, whereas  
226 deprotonation in alkaline conditions dissolves fatty acids or promotes micelle formation. Under  
227 alkaline hydrothermal conditions, fatty acids are well above their pK<sub>a</sub>, hence all carboxylic acid  
228 headgroups deprotonate, favouring dissolution<sup>47</sup>. Lengthening the fatty-acid chains raises the  
229 apparent pK<sub>a</sub> through hydrophobic interactions between their tails<sup>52,53</sup>, but this effect is limited.  
230 Adding 1-alkanols strongly promotes vesicle formation as the alcohol headgroups do not  
231 deprotonate<sup>37,55</sup>. A 1:1 mixture of fatty acids and 1-alkanols therefore forms vesicles at high pH as  
232 the headgroups of the two species are equally protonated and deprotonated, forming stable  
233 hydrogen bonds even in strongly alkaline conditions (Fig. 2).

234           The standard lab procedure to promote vesicle self-assembly begins with deprotonated fatty  
235 acids at high pH, to ensure that amphiphiles are in solution or micellar form<sup>47</sup>. The pH is then titrated  
236 down to the apparent pKa, whereupon vesicles self-assemble. In other words, vesicles do not form  
237 spontaneously at lower pH, but initially require strongly alkaline pH to self-assemble. While it is  
238 possible to form vesicles without raising the pH, we note that this can be achieved only after adding  
239 NaOH in the presence of buffer. In the absence of buffers, alkaline conditions are necessary to first  
240 deprotonate and dissolve fatty acids. We have observed that simply adding SCAs to salty water at pH  
241 7 does not form vesicles, as the fatty acids are mostly protonated and form an emulsion of lipid  
242 droplets rather than bilayer vesicles. Once deprotonated and dissolved under alkaline conditions,  
243 titration down to more acidic conditions, as in the lab procedure, now forms bilayer vesicles. This  
244 titration would occur naturally by mixing with mildly acidic ocean waters in Hadean vents<sup>56</sup>, and  
245 does not disassemble vesicles except at pH below 6.5 (though earlier work shows that vesicles can  
246 also form even at strongly acidic pH<sup>42,45</sup>). With more complex mixtures of fatty acids and 1-alkanols,  
247 there is no need to titrate with acid to form vesicles, as they form spontaneously even above pH 12,  
248 even in the absence of salts. Initial heating is needed for similar reasons. Vesicles do not form readily  
249 from solid fatty acids below their melting point (or when protonated, as noted above). The melting  
250 point of fatty acids and 1-alkanols depends on chain length, with C<sub>15</sub> fatty acids melting around 53  
251 °C. To dissolve long-chain SCAs therefore requires temperatures similar to those found in alkaline  
252 hydrothermal vents (typically 50-90 °C)<sup>34,50,51</sup>; we used 70 °C. Once formed at warm temperatures,  
253 vesicles are still present on cooling (Supplementary Fig. 12), again consistent with mixing in the vents  
254 with cooler ocean waters. Far from precluding protocell formation, the pH and temperature range in  
255 alkaline hydrothermal vents should therefore promote their self-assembly at the origin of life.

256           Salinity is also known to promote vesicle assembly through both polar (electrical shielding of  
257 the charged headgroups) and non-polar (more pronounced phase partitioning of hydrophobic tails)  
258 effects<sup>42,54</sup>. Nonetheless, earlier work concluded that high salt concentrations (>150 mM) disrupt  
259 vesicle formation and would preclude the formation of protocells at modern ocean salinity (~600

260 mM NaCl)<sup>37-41</sup>. If the salinity of Hadean oceans were equivalent, this reasoning goes, then life could  
261 not have begun in the oceans and must have started in terrestrial freshwater pools. The inferred  
262 salinity of Hadean oceans is difficult to constrain. Extrapolations based on fluid inclusions trapped in  
263 ancient rocks are questionable<sup>57</sup>, but three factors are pertinent: (i) acid leaching of the crust by hot  
264 early oceans should have released Na<sup>+</sup> into the oceans rapidly, so that maximum salinity was  
265 reached quickly<sup>57</sup>; (ii) the lack of evaporitic salt deposits in the Hadean, given practically global  
266 oceans, means that Hadean oceans could have had nearly double the salt content of modern  
267 oceans<sup>58</sup>; but (iii) the sequestration of water as hydrated minerals (e.g. serpentinites) over 4.5 billion  
268 years means that Hadean oceans could have had twice the volume of modern oceans<sup>59-61</sup>. A  
269 conservative position is therefore that ocean salinity was similar to today. If life started in the  
270 oceans, then protocells would need to tolerate ~600 mM NaCl.

271         The difficulty of forming vesicles at modern ocean salinity reported by others can best be  
272 ascribed to the use of simple mixtures of largely C<sub>10</sub> SCAs. We show that more complex mixtures of  
273 12 C<sub>10</sub>-C<sub>15</sub> fatty acids and 1-alkanols do indeed form numerous individual vesicles at modern ocean  
274 salinity (Fig. 5). Higher salinity sometimes promotes the aggregation of vesicles or the formation of  
275 filamentous structures observed by confocal microscopy (Fig. 6) and certainly there are fewer  
276 individual vesicles under these conditions. However, NS-TEM analysis suggests that these filaments  
277 are composed entirely of individual SCA vesicles (Fig. 6). The vesicles burst under vacuum, so appear  
278 collapsed during microscopy. Similar structures have been found in liposome research previously (by  
279 both confocal microscopy and NS-TEM, as reported here) and are known to be metastable<sup>62-64</sup>. More  
280 work is needed to characterise these remarkable structures and elucidate their chemical properties  
281 in an origin-of-life context.

282         Divalent cations, notably Mg<sup>2+</sup> and Ca<sup>2+</sup>, have also been shown to disrupt vesicle  
283 formation<sup>39,40</sup>. Their concentration in Hadean oceans is unknown, and estimates vary greatly<sup>65,66</sup>.  
284 Ocean levels are in any case a poor surrogate for vent systems; the concentration of Ca<sup>2+</sup> and Mg<sup>2+</sup> in  
285 modern alkaline vent fluids is extremely variable, with some features containing no Ca<sup>2+</sup> or Mg<sup>2+</sup> at

286 all<sup>67</sup>. We therefore examined vesicle stability in the presence of modern seawater concentrations of  
287  $Mg^{2+}$  and  $Ca^{2+}$ , as earlier work reported that seawater levels aggregate fatty acid/1-alkanol vesicles  
288 into insoluble curds<sup>39,40</sup>. While simple organic chelators such as citrate can prevent this from  
289 happening<sup>68</sup> (and vesicles composed of decylamine and decanoic acid have been shown to form in  
290 the presence of 0.1 M  $Mg^{2+}$  and  $Ca^{2+}$  salts<sup>44</sup>) we find that alkaline pH alone offers some protection.  
291 Divalent cations form complexes with amphiphile head groups at low pH, prohibiting bilayer  
292 formation and producing soapy solutions<sup>36-41,47,55</sup>. In contrast, strongly alkaline conditions favour  
293 hydroxide complexes with these inorganic ions, in effect rendering them unavailable for vesicle  
294 disruption. Plentiful vesicles form at strongly alkaline pH (pH 11-12) in the presence of 50 mM  $Mg^{2+}$   
295 and 10 mM  $Ca^{2+}$  (Fig. 5) but very few form at pH <9 (Supplementary Fig. 7). While the combination of  
296 modern seawater concentrations of NaCl,  $Mg^{2+}$  and  $Ca^{2+}$  at pH 11 and 70 °C did disrupt vesicle  
297 formation with mixtures of 12 C<sub>10</sub>-C<sub>15</sub> fatty acids and 1-alkanols, addition of two C<sub>10</sub> isoprenoids,  
298 geranic acid and geraniol enabled vesicle assembly even under these most extreme conditions, as  
299 demonstrated by confocal microscopy, cryo-TEM (Fig. 7) and NS-TEM (Extended Data Fig. 9 and  
300 Supplementary Figs. 8-10). We confirmed the stability of these vesicles in oceanic alkaline  
301 hydrothermal conditions through encapsulation of the fluorescent dye pyranine (Fig. 3). We explore  
302 the reasons for this increased stability elsewhere<sup>69</sup>.

303 We conclude that deep-sea alkaline hydrothermal conditions in the Hadean should have  
304 promoted the synthesis of long-chain amphiphiles and their self-assembly into protocells at the  
305 origin of life. Thermophoresis<sup>26</sup> and interactions with mineral surfaces in porous vents<sup>27</sup> concentrate  
306 amphiphiles above the critical bilayer concentration. Vents sustain the moderately high  
307 temperatures needed to ensure that longer chain amphiphiles are above their melting point and so  
308 available for vesicle formation in solution<sup>41</sup>. Alkaline pH is essential to dissolve the SCAs in water,  
309 deprotonating the head-groups of some amphiphiles and reducing the concentration of divalent  
310 cations such as  $Ca^{2+}$  and  $Mg^{2+}$  in solution. Titration by mixing with more acidic ocean waters within  
311 vents favours vesicle self-assembly. Salts promote vesicle assembly<sup>41</sup> as well as aggregation of three-

312 dimensional structures that could potentially harness geologically sustained pH gradients to drive  
313 CO<sub>2</sub> fixation<sup>29,70,71</sup>. Mixtures of amphiphiles are geochemically<sup>21</sup> and biochemically<sup>72</sup> meaningful, and  
314 are critical to forming protocells capable of growth and simple heredity<sup>29</sup> at the origin of life.

315

## 316 **Methods**

### 317 **Materials**

318 Decanoic acid, dodecanoic acid, tetradecanoic acid, decan-1-ol, undecan-1-ol and geraniol were  
319 purchased from Acros Organics. Undecanoic acid, tridecanoic acid, tridecan-1-ol, geranic acid,  
320 sodium chloride (NaCl), calcium chloride dihydrate (CaCl<sub>2</sub>·2H<sub>2</sub>O), Sephadex G-50 and 8-  
321 hydroxypyrene-1,3,6-trisulfonic acid (pyranine) were purchased from Sigma Aldrich. Pentadecanoic  
322 acid, dodecan-1-ol, tetradecan-1-ol, pentadecan-1-ol and magnesium chloride hexahydrate  
323 (MgCl<sub>2</sub>·6H<sub>2</sub>O) were purchased from Alfa Aesar. All reagents used were analytical grade (≥ 97%).

324

### 325 **Preparation of vesicle solutions**

326 All laboratory work was carried out in a dry heat block (SciQuip HP120-S) at 70 °C. Density values for  
327 each compound at this temperature were obtained gravimetrically (Supplementary Table 2). Vesicle  
328 solutions were prepared daily following a modified version of the procedure outlined by Monnard  
329 and Deamer<sup>47</sup>. Buffers were not employed in any solutions in an effort to maintain prebiotic  
330 relevance. A 7 mL 10 mM stock solution of vesicles was prepared by adding equimolar  
331 concentrations of each fatty acid to 4 mL of deionised H<sub>2</sub>O in a glass vial. The pH was adjusted to >12  
332 with 500 µL 1 M NaOH and the solution was vortexed to ensure full dissolution of deprotonated  
333 acids. For vesicles containing 1-alkanols, equimolar concentrations were added at this stage and the  
334 solution was vortexed. The solution was then brought to a final volume of 7 mL with 1 M NaOH (final  
335 pH ~12). 500 µL of the stock solution was added to a fresh glass vial. The solution was titrated with  
336 gradual addition of 1 M HCl followed by pH measurement (Fisher Scientific accumet AE150 meter  
337 with VWR semi-micro pH electrode) to achieve the desired pH. The solution was brought to a final

338 volume of 1 mL with deionised H<sub>2</sub>O resulting in a concentration of 5 mM after which the pH value  
339 was recorded. For isoprenoid-containing solutions, isoprenoid acids and alcohols were added in  
340 conjunction with fatty acids and 1-alkanols respectively.

341 For critical bilayer concentration (CBC) experiments, the same procedure was used followed  
342 by serial dilution in order to obtain the desired concentrations. The pH of each solution was  
343 measured again prior to analysis. In order to test the influence of NaCl, Mg<sup>2+</sup>, and Ca<sup>2+</sup>, this  
344 procedure was carried out using aqueous solutions of the desired salt concentration in the place of  
345 H<sub>2</sub>O. Identical quantities of salts were dissolved in 1M NaOH and 1M HCl for use in pH adjustment,  
346 thereby ensuring that the concentration of salt remained constant throughout the experiment.

347

#### 348 **Determination of vesicle formation and CBC**

349 Optical density (OD) measurements were obtained by measuring absorbance at 480 nm on an  
350 Infinite M200 Pro Spectrophotometer (Tecan) and data was processed using the Magellan software  
351 package. Three 50 µL aliquots of each solution were transferred to separate wells on a Falcon black  
352 96 well plate (pre-heated to 70 °C) and immediately analysed. The instrument was set to 30 °C and  
353 the plate was shaken for 10 s before analysis. To determine the pH range of vesicle formation data  
354 from multiple solutions were collated and a plot of pH versus absorbance was prepared. Minimal OD  
355 values indicate the presence of micelles. As the SCAs are gradually protonated, vesicles begin to  
356 form and the OD increases. Maximum values are obtained once SCAs become fully protonated and  
357 begin to form droplets as opposed to vesicles (Extended Data Fig. 1). To allow for better data  
358 visualisation and comparison, values in Figure 1 were normalised and fit to a sigmoid model  
359 representing the phase transition of the solutions. The initial upward turning point of the curve was  
360 defined as the transition point whereby vesicle formation begins. Interpretations made based on  
361 these plots were confirmed by confocal and electron microscopy.

362 CBC was also determined by OD measurement. Solutions were prepared in a range of  
363 concentrations and analysed as previously described. Data were interpreted following the same

364 procedure as Maurer and Nguyen<sup>54</sup>. A linear function was fit through baseline values and through  
365 increasing values. The point of intersection of these two lines corresponds to the CBC and was  
366 determined algebraically.

367

#### 368 **Encapsulation and release of pyranine dye**

369 Encapsulation capacity of vesicles was determined by preparation of solutions in the presence of 10  
370  $\mu\text{M}$  pyranine dye. All solutions were maintained at 70 °C during the procedure. A 200  $\mu\text{L}$  aliquot of  
371 the solution was then separated by size exclusion chromatography using a glass column (30 x 1 cm)  
372 filled with Sephadex G-50 medium beads. Fractions (3 drops,  $\sim 130 \mu\text{L}$  total) were collected in a  
373 Falcon black 96-well plate and analysed immediately. Encapsulation was measured by fluorescence  
374 spectroscopy on an Infinite M200 Pro spectrophotometer (Tecan) using excitation and emission  
375 wavelengths of 450 and 508 nm respectively. Data were processed using the Magellan software  
376 package. Vesicle fractions were combined and separated again by size exclusion chromatography  
377 after 24 hours to determine release of pyranine over time.

378

#### 379 **Confocal microscopy**

380 Confocal microscopy of vesicle solutions was performed on a Zeiss LSM-T-PMT with an Ar laser at  
381 514 nm coupled to an Airyscan detector. 0.5  $\mu\text{L}$  of 100  $\mu\text{M}$  rhodamine-6G was added to a heated  
382 glass slide followed by 5  $\mu\text{L}$  of sample solution. These were mixed on the slide and covered with a  
383 heated coverslip. Images were captured using a 63X oil objective.

384

#### 385 **Negative-staining Transmission Electron Microscopy (NS-TEM)**

386 Samples were analysed by TEM using a negative staining (NS-TEM) method. A drop of sample  
387 solution was applied to a copper TEM grid and allowed to stand for 1 minute. Excess sample was  
388 removed by blotting with filter paper. An aliquot of 1.5% aqueous uranyl acetate solution was



389 applied to the grid for a further 1 minute and the excess was subsequently removed with filter  
390 paper. Samples were analysed immediately on a JEOL 1010 TEM (JEOL, Japan).

391

### 392 **Cryogenic TEM**

393 Samples were applied directly to glow-discharged Lacey Carbon (400 mesh Cu) grids (Agar Scientific)  
394 for 30 s, blotted for 8.5 or 11 s at 4.5 °C and 95% humidity, and then rapidly plunged into liquid  
395 ethane using a Vitrobot Mark IV (Thermo Fisher). Imaging was completed using a T10 microscope  
396 (FEI) operated at 100 kV. Images were collected at a magnification range of 7000-34000x.

397

### 398 **Data availability**

399 All data are available in the main text, Extended Data Figs. 1-10 and Supplementary Information  
400 (Supplementary Materials and Methods, Supplementary Figs. 1-14 and Supplementary Tables 1-2.

401

### 402 **Competing interests statement**

403 The authors declare no competing interests.

404

### 405 **Acknowledgements**

406 We thank Mark Turmaine for assistance with NS-TEM, and Prof Beppe Battaglia, Prof Finn Werner  
407 and Prof Don Braben for valuable discussions. We would like to thank the anonymous reviewers  
408 whose input significantly improved the manuscript. We are grateful to the BBSRC (HR, LIDo Doctoral  
409 Training Programme) and bgc3 for funding. A.M.H and A.M. are funded by the Medical Research  
410 Council U.K. (Career Development Award MR/M00936X/1 to A.M.).

411

### 412 **Author contributions**

413 NL supervised the work; SFJ, HR, INZ, AMH, AM and NL conceived and designed the experiments;  
414 SFJ, HR, INZ & AMH performed the experiments; SFJ, INZ, AMH & AM contributed materials and  
415 analysis tools; SFJ & NL analysed the data; SFJ and NL wrote the paper.

416

#### 417 **References**

- 418 Mitchell, P. in *Proceedings of the first International Symposium on the Origin of Life on the Earth,*  
419 *held at Moscow, 19-24 August 1957 (I.U.B. symposium series)* 437–443 (1959).
- 420 Nitschke, W. & Russell, M. J. Hydrothermal focusing of chemical and chemiosmotic energy,  
421 supported by delivery of catalytic Fe, Ni, Mo/W, Co, S and Se, forced life to emerge. *J. Mol.*  
422 *Evol.* **69**, 481–496 (2009).
- 423 Fuchs, G. Alternative pathways of carbon dioxide fixation: Insights into the early evolution of  
424 life? *Annu. Rev. Microbiol.* **65**, 631–658 (2011).
- 425 Lane, N. & Martin, W. F. The origin of membrane bioenergetics. *Cell* **151**, 1406–1416 (2012).
- 426 Mulkidjanian, A. Y., Galperin, M. Y. & Koonin, E. V. Co-evolution of primordial membranes and  
427 membrane proteins. **34**, 206–215 (2009).
- 428 Koga, Y., Kyuragi, T., Nishihara, M. & Sone, N. Did archaeal and bacterial cells arise independently  
429 from noncellular precursors? A hypothesis stating that the advent of membrane phospholipid with  
430 enantiomeric glycerophosphate backbones caused the separation of the two lines of descent. *J. Mol.*  
431 *Evol.* **46**, 54–63 (1998).
- 432 Martin, W. & Russell, M. J. On the origins of cells: a hypothesis for the evolutionary transitions from  
433 abiotic geochemistry to chemoautotrophic prokaryotes, and from prokaryotes to nucleated  
434 cells. *Philos. Trans. R. Soc. B Biol. Sci.* **358**, 59–85 (2003).
- 435 Koga, Y. Early evolution of membrane lipids: How did the lipid divide occur? *J. Mol. Evol.* **72**, 274–282  
436 (2011).
- 437 Sojo, V. On the biogenic origins of homochirality. *Orig. Life Evol. Biosph.* **45**, 219–224 (2015).

438 Lombard, J., López-García, P. & Moreira, D. The early evolution of lipid membranes and the three  
439 domains of life. *Nat. Rev. Microbiol.* **10**, 507–515 (2012).

440 Shimada, H. & Yamagishi, A. Stability of heterochiral hybrid membrane made of bacterial sn-G3P  
441 lipids and archaeal sn-G1P lipids. *ACS Biochem.* **50**, 4114–4120 (2011).

442 Caforio, A., Siliakus, M. F., Exterkate, M., Jain, S. & Jumde, V. R. Converting *Escherichia coli* into an  
443 archaeobacterium with a hybrid heterochiral membrane. *PNAS* **115**, 3705–3709 (2018).

444 Hanczyc, M. M. & Szostak, J. W. Replicating vesicles as models of primitive cell growth and  
445 division. *Curr. Opin. Chem. Biol.* **8**, 660–664 (2004).

446 Chen, I. A. & Szostak, J. W. Membrane growth can generate a transmembrane pH gradient in fatty  
447 acid vesicles. *PNAS* **101**, 7965–7970 (2004).

448 Chen, I. A. & Szostak, J. W. A kinetic study of the growth of fatty acid vesicles. *Biophys. J.* **87**, 988–  
449 998 (2004).

450 Sojo, V., Pomiankowski, A. & Lane, N. A bioenergetic basis for membrane divergence in archaea and  
451 bacteria. *PLoS Biol.* **12**, e1001926 (2014).

452 Segré, D., Ben-Eli, D., Deamer, D. W. & Lancet, D. The lipid world. *Orig. Life Evol. Biosph.* **31**, 119–145  
453 (2001).

454 Segré, D., Ben-Eli, D. & Lancet, D. Compositional genomes: Prebiotic information transfer in mutually  
455 catalytic noncovalent assemblies. *PNAS* **97**, 4112–4117 (2000).

456 Amend, J. P. & McCollom, T. M. Energetics of biomolecule synthesis on early earth. *ACS Symp.*  
457 *Ser.* **1025**, 63–94 (2009).

458 Martin, W. Carbon-metal bonds: rare and primordial in metabolism. *Trends Biochem. Sci.* **44**, 807–  
459 818 (2019).

460 McCollom, T. M., Ritter, G. & Simoneit, B. R. T. Lipid synthesis under hydrothermal conditions  
461 by Fischer-Tropsch reactions. *Orig. life Evol. Biosph.* **29**, 153–166 (1999).

462 Scheidler, C., Sobotta, J., Eisenreich, W., Wächtershäuser, G. & Huber, C. Unsaturated C<sub>3,5,7,9</sub>-  
463 monocarboxylic acids by aqueous, one-pot carbon fixation: possible relevance for the origin of  
464 life. *Sci. Rep.* **6**, 27595 (2016).

465 Decker, P. & Schweer, H. Reactions in the formol bioid: the origin of branched chains of isoprenoids,  
466 valine, and leucines. *Orig. Life* **14**, 335–342 (1984).

467 Prey, H. A., Schweickert, C. E. & Minnich, B. H. Solubility of hydrogen, oxygen, nitrogen, and helium  
468 in water. *Ind. Eng. Chem.* **44**, 1146–1151 (1952).

469 Baaske, P. *et al.* Extreme accumulation of nucleotides in simulated hydrothermal pore systems. *Proc.*  
470 *Natl. Acad. Sci.* **104**, 9346–9351 (2007).

471 Budin, I., Bruckner, R. J. & Szostak, J. W. Formation of protocell-like vesicles in a thermal diffusion  
472 column. *J.A.C.S Commun.* **131**, 9628–9629 (2009).

473 Hanczyc, M. M., Mansy, S. S. & Szostak, J. W. Mineral surface directed membrane assembly. *Orig.*  
474 *Life Evol. Biosph.* **37**, 67–82 (2007).

475 Buckel, W. & Thauer, R. K. Flavin-based electron bifurcation, ferredoxin, flavodoxin, and anaerobic  
476 respiration with protons (Ech) or NAD<sup>+</sup> (Rnf) as electron acceptors: a historical review. *Front.*  
477 *Microbiol.* **9**, 401 (2018).

478 West, T., Sojo, V., Pomiankowski, A. & Lane, N. The origin of heredity in protocells. *Philos. Trans. R.*  
479 *Soc. B Biol. Sci.* **372**, 20160419 (2017).

480 Russell, M. J. & Hall, A. J. The emergence of life from iron monosulphide bubbles at a submarine  
481 hydrothermal redox and pH front. *J. Geol. Soc. London.* **154**, 377–402 (1997).

482 Russell, M. J. & Martin, W. The rocky roots of the acetyl-CoA pathway. *Trends Biochem. Sci.* **29**, 358–  
483 363 (2004).

484 Russell, M. J., Daniel, R. M., Hall, A. J. & Sherringham, J. A hydrothermally precipitated catalytic iron  
485 sulphide membrane as a first step toward life. *J. Mol. Evol.* **39**, 231–243 (1994).

486 Martin, W. & Russell, M. J. On the origin of biochemistry at an alkaline hydrothermal vent. *Philos.*  
487 *Trans. R. Soc. Lond. B. Biol. Sci.* **362**, 1887–1925 (2007).

~~488~~ Martin, W., Baross, J., Kelley, D. & Russell, M. J. Hydrothermal vents and the origin of life. *Nat. Rev.*  
489 *Microbiol.* **6**, 805–814 (2008).

~~490~~ Russell, M. J. *et al.* The drive to life on wet and icy worlds. *Astrobiology* **14**, 308–343 (2014).

~~491~~ Monnard, P.-A., Apel, C. L., Kanavarioti, A. & Deamer, D. W. Influence of ionic inorganic solutes on  
492 self-assembly and polymerization processes related to early forms of life: implications for a prebiotic  
493 aqueous medium. *Astrobiology* **2**, 139–152 (2002).

~~494~~ Monnard, P. A. & Deamer, D. W. Membrane self-assembly processes: Steps toward the first cellular  
495 life. *Anat. Rec.* **207**, 123–151 (2002).

~~496~~ Szostak, J. W., Bartel, D. P. & Luisi, P. L. Synthesizing life. *Nature* **409**, 387–390 (2001).

~~497~~ Deamer, D. The role of lipid membranes in life's origin. *Life* **7**, 5 (2017).

~~498~~ Milshteyn, D, Damer, B., Havig, J. & Deamer, D. Amphiphilic compounds assemble into membranous  
499 vesicles in hydrothermal hot spring water but not in seawater. *Life* **8**, 11 (2018).

~~500~~ Maurer, S. The impact of salts on single chain amphiphile membranes and implications for the  
501 location of the origin of life. *Life* **7**, 44 (2017).

~~502~~ Maurer, S. E. *et al.* Vesicle self-assembly of monoalkyl amphiphiles under the effects of high ionic  
503 strength, extreme pH, and high temperature environments. *Langmuir* **34**, 15560–68 (2018).

~~504~~ Apel, C. L., Deamer, D. W. & Mautner, M. N. Self-assembled vesicles of monocarboxylic acids and  
505 alcohols: conditions for stability and for the encapsulation of biopolymers. *Biochim. Biophys. Acta*  
506 **1519**, 1–9 (2002).

~~507~~ Rendón, A., Gil Carton, D., Sot, J., García-Palacios, M., Montes, R., Valle, M., Arrondo, J-L. R., Goñi,  
508 F.M. & Ruiz-Mirazo, K. Model systems of precursor cellular membranes: long-chain alcohols stabilize  
509 spontaneously formed oleic acid vesicles. *Biophys. J.* **102**, 278–286 (2012).

~~510~~ Namani, T. & Deamer, D. W. Stability of model membranes in extreme environments. *Orig. Life Evol.*  
511 *Biosph.* **38**, 329–341 (2008).

5162 Cape, J. L., Monnard, P. A. & Boncella, J. M. Prebiotically relevant mixed fatty acid vesicles support  
513 anionic solute encapsulation and photochemically catalyzed trans-membrane charge transport.  
514 *Chem. Sci.* **2**, 661–671 (2011).

515 Monnard, P. A. & Deamer, D. W. Preparation of vesicles from nonphospholipid amphiphiles.  
516 *Methods Enzymol.* **372**, 133–151 (2003).

517 Thanh Thuy, D., Decnop-Weever, D., Th. Kok, W., Luan, P. & Vong Nghi, T. Determination of traces of  
518 calcium and magnesium in rare earth oxides by flow-injection analysis. *Anal. Chim. Acta* **295**, 151–  
519 157 (1994).

520 Avnir, Y. & Barenholz, Y. pH determination by pyranine: medium-related artifacts and their  
521 correction. *Anal. Biochem.* **347**, 34–41 (2005).

522 Kelley, D. S. *et al.* An off-axis hydrothermal vent field near the Mid-Atlantic Ridge at 30 degrees  
523 N. *Nature* **412**, 145–149. (2001).

524 Kelley, D. S. *et al.* A serpentinite-hosted ecosystem: The Lost City hydrothermal  
525 field. *Science* **307**, 1428–1434 (2005).

526 Smith, R. & Tanford, C. Hydrophobicity of long chain n-alkyl carboxylic acids, as measured by their  
527 distribution between heptane and aqueous solutions. *PNAS* **70**, 289–293 (1973).

528 Budin, I., Prywes, N., Zhang, N. & Szostak, J. W. Chain-length heterogeneity allows for the assembly  
529 of fatty acid vesicles in dilute solution. *Biophys. J.* **107**, 1582–90 (2014).

530 Maurer, S. E. & Nguyen, G. Prebiotic vesicle formation and the necessity of salts. *Orig. Life Evol.*  
531 *Biosph.* **46**, 215–222 (2016).

532 Hargreaves, W. R. & Deamer, D. W. Liposomes from ionic, single-chain amphiphiles.  
533 *Biochemistry* **17**, 3759–3768 (1978).

534 Sojo, V., Herschy, B., Whicher, A., Camprubí, E. & Lane, N. The origin of life in alkaline hydrothermal  
535 vents. *Astrobiology* **16**, 181–197 (2016).

536 Marty, B., Avice, G., Bekaert, D. V & Broadley, M. W. Salinity of the Archaean oceans from analysis of  
537 fluid inclusions in quartz. *Comptes rendus - Geosci.* **350**, 154–163 (2018).

538 Holland, H. D. *The Chemical Evolution of the Atmosphere and Oceans*. (Princeton University Press,  
539 1984).

540 Fyfe, W. S. The water inventory of the Earth: fluids and tectonics. *Geological Soc. Spec. Publ.* **78**, 1–7  
541 (1994).

542 Arndt, N. T. & Nisbet, E. G. Processes on the young earth and the habitats of early life. *Annu. Rev.*  
543 *Earth Planet. Sci.* **40**, 521–549 (2012).

544 Russell, M. J. & Arndt, N. T. Geodynamic and metabolic cycles in the Hadean. *Biogeosciences* **2**, 97–  
545 111 (2005).

546 Lopresti, C., Lomas, H., Massignani, M., Smart, T. & Battaglia, G. Polymersomes: nature inspired  
547 nanometer sized compartments. *J. Mater. Chem.* **19**, 3576–3590 (2009).

548 Smart, T. *et al.* Block copolymer nanostructures. *Nanotoday* **3**, 38–46 (2008).

549 Bonaccio, S., Wessicken, M., Berti, D., Walde, P. & Luisi, P. L. Relation between the molecular  
550 structure of phosphatidyl nucleosides and the morphology of their supramolecular and mesoscopic  
551 aggregates. *Langmuir* **12**, 4976–4978 (1996).

552 Morse, J. W. & Mackenzie, F. T. Hadean ocean carbonate geochemistry. *Aquat. Geochemistry* **4**,  
553 301–319 (1998).

554 Holm, N. G. The significance of Mg in prebiotic geochemistry. *Geobiology* **10**, 269–279 (2012).

555 Ludwig, K. A., Kelley, D. S., Butterfield, D. A., Nelson, B. K. & Fru-Green, G. Formation and evolution  
556 of carbonate chimneys at the Lost City Hydrothermal Field. *Geochim. Cosmochim. Acta* **70**, 3625–  
557 3645 (2006).

558 Adamala, K. & Szostak, J. W. Nonenzymatic template-directed RNA synthesis inside model  
559 protocells. *Science* **342**, 1098–1101 (2013).

560 Jordan, S. F., Nee, E., & Lane, N. Isoprenoids enhance the stability of fatty acid membranes at the  
561 emergence of life potentially leading to an early lipid divide. *Interface Focus* 20190067 (2019).

562 Camprubi, E., Jordan, S. F., Vasiliadou, R. & Lane, N. Iron catalysis at the origin of life. *IUBMB*  
563 *Life* **69**, 373–381 (2017).

564 Lane, N., Allen, J. F. & Martin, W. How did LUCA make a living? Chemiosmosis in the origin of  
565 life. *BioEssays* **32**, 271–280 (2010).

566 Harrison, S. & Lane, N. Life as a guide to prebiotic nucleotide synthesis. *Nat. Commun.* **9**, 5176  
567 (2018).

568

569



570 **Figure legends**

571

572 **Figure 1.** Plots of normalised absorbance at 480 nm versus pH, with corresponding confocal  
573 micrographs for the transition point from the micellar to vesicular phase, for 50 mM C<sub>10</sub> fatty acid  
574 (a), 5 mM C<sub>10</sub>-C<sub>15</sub> fatty acid mixture (b), and 5 mM 5:1 C<sub>10</sub>-C<sub>15</sub> fatty acid/1-alkanol mixture (c). Error  
575 bars in (a), (b), and (c) represent the standard deviation (n = 3).

576

577 **Figure 2.** Plot of absorbance at 480 nm versus pH for 5 mM 1:1 C<sub>10</sub>-C<sub>15</sub> fatty acid/1-alkanol mixture  
578 (a) with corresponding confocal micrographs at pH 7.09 (b), pH 10.45 (c), and pH 12.13 (d). Error  
579 bars in (a) represent the standard deviation (n = 3).

580

581 **Figure 3.** (a) Encapsulation of the fluorescent dye pyranine, showing a peak for pyranine  
582 encapsulated within vesicles composed of 5 mM 1:1 C<sub>10</sub>-C<sub>15</sub> fatty acid/1-alkanol mixture at FN ~20,  
583 and a larger peak for free dye at FN ~70. (b) Vesicles as in (a) but after 24 h encapsulation, with  
584 ~20% of the encapsulated pyranine peak remaining at FN ~20. (c) and (d) Equivalent plots for the full  
585 5 mM 1:1:1 C<sub>10</sub>-C<sub>15</sub> fatty acid/1-alkanol/C<sub>10</sub> isoprenoid mixture. (e) Fluorescence from free pyranine  
586 in water (solid line) and water with full salt solution at pH 12 (dotted line), showing interaction of  
587 dye with salt mixture leading to a substantially lower free pyranine peak after chromatography. (f)  
588 Encapsulation of pyranine in vesicles composed of 5 mM 1:1:1 C<sub>10</sub>-C<sub>15</sub> fatty acid/1-alkanol/C<sub>10</sub>  
589 isoprenoid mixture, with encapsulated pyranine fluorescence at FN ~20 and free dye at FN ~70. Note  
590 log scale on Y axis to emphasise encapsulation despite disruption from salt interactions. Pink shading  
591 in (a) and (c) represents the standard deviation (n = 3).

592

593 **Figure 4.** a Plot of absorbance at 480 nm versus concentration for C<sub>10</sub>-C<sub>15</sub> fatty acid mixture at pH ~8  
594 and C<sub>10</sub> fatty acid at pH ~7 showing calculated critical bilayer concentrations (CBC) of 1.35 mM and  
595 39 mM respectively (with each individual FA present at 225 μM). Error bars represent the standard

596 deviation ( $n = 3$ ). **b** Cryo-TEM micrograph of 600  $\mu\text{M}$  1:1  $\text{C}_{10}\text{-C}_{15}$  fatty acid/alcohol mixture at pH 7.71  
597 (with each individual FA present at 100  $\mu\text{M}$ ).

598

599 **Figure 5.** Confocal micrographs of 5 mM 1:1  $\text{C}_{10}\text{-C}_{15}$  fatty acid/alcohol mixture in 600 mM NaCl pH  
600 11.17 (**a**), 50 mM  $\text{MgCl}_2$  pH 11.65 (**b**), and 10 mM  $\text{CaCl}_2$  pH 11.84 (**c**) along with corresponding Cryo-  
601 TEM micrographs at pH 12.17 (**d**), pH 12.31 (**e**), and pH 12.29 (**f**).

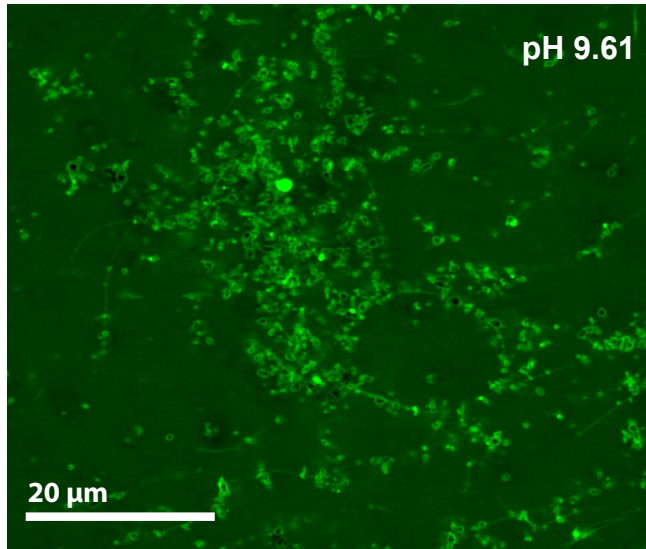
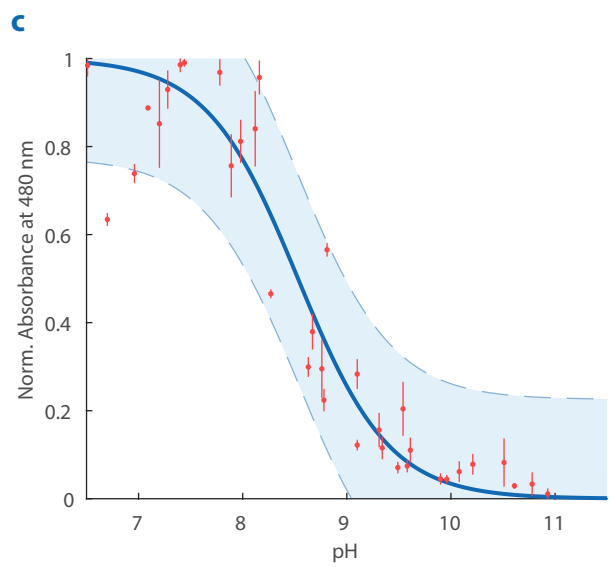
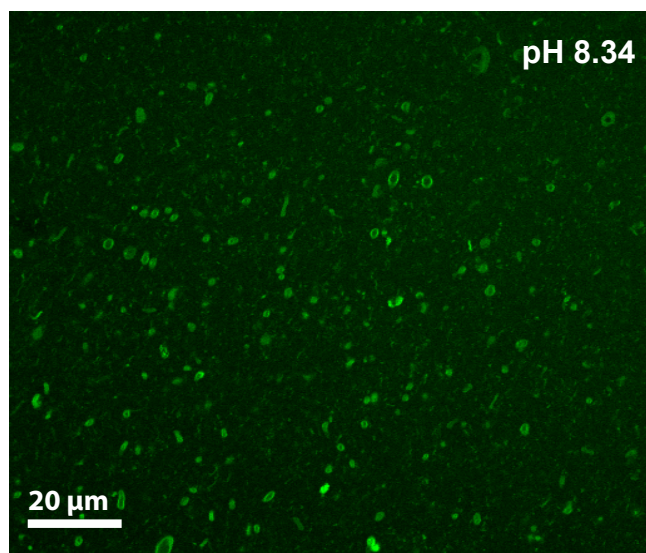
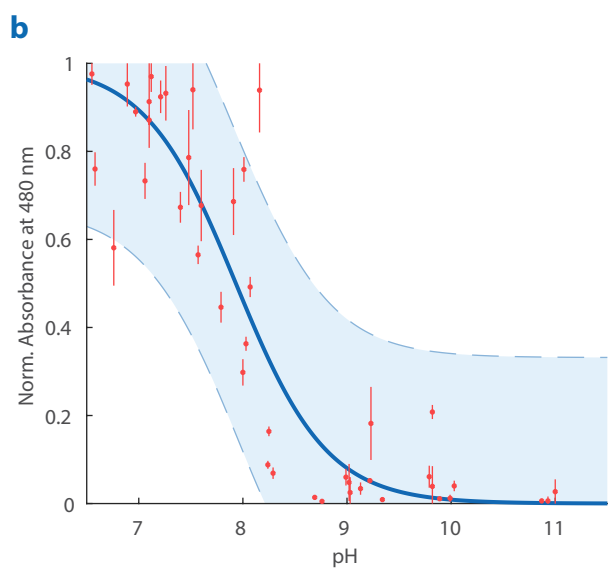
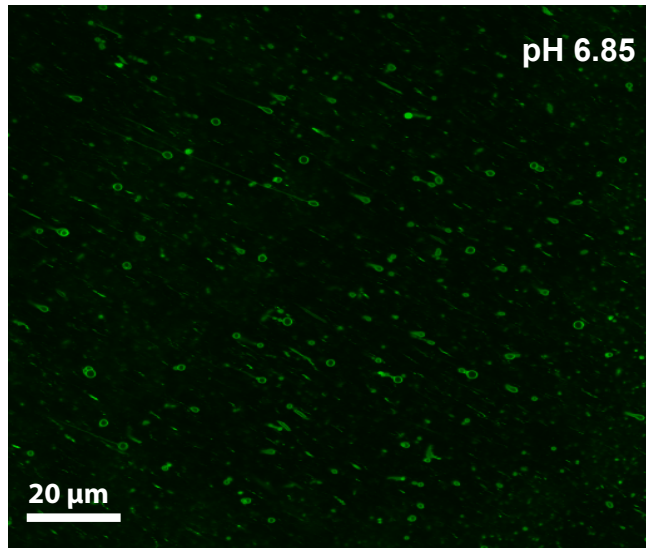
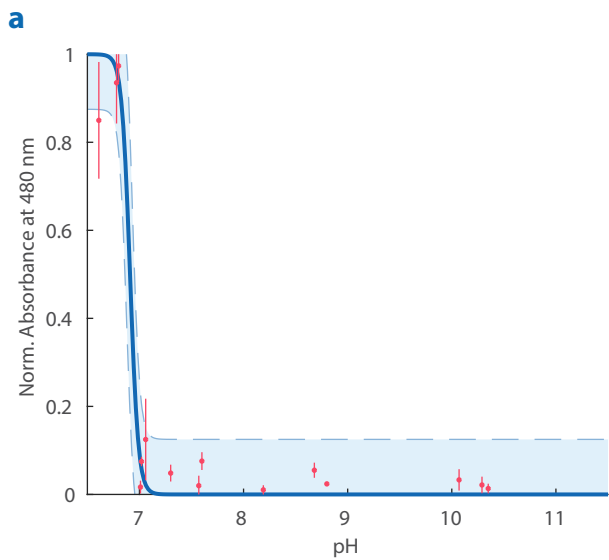
602

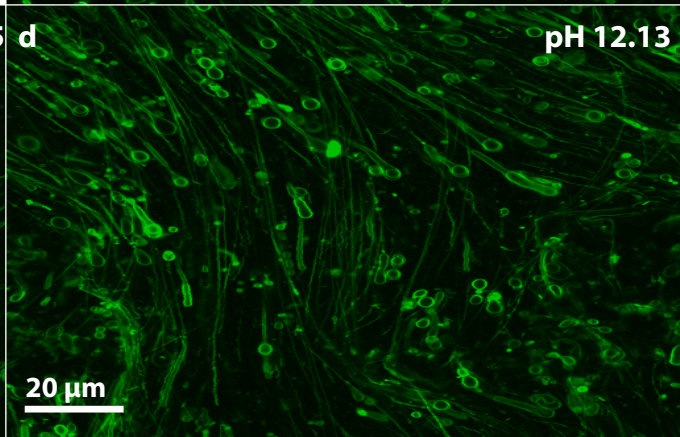
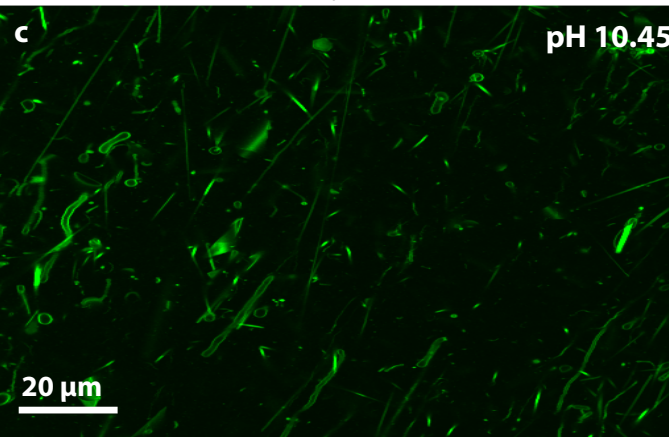
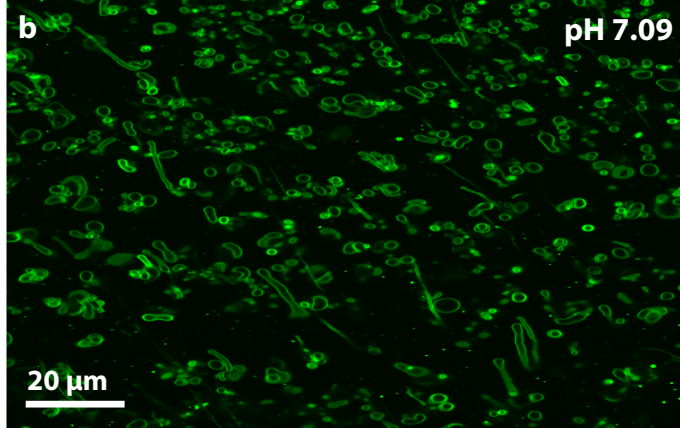
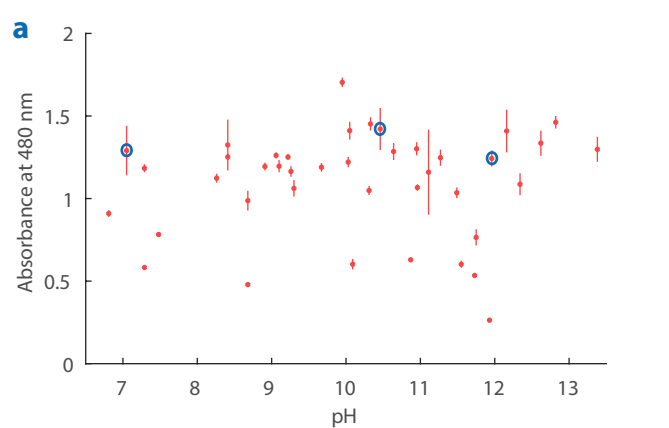
603 **Figure 6.** Filamentous vesicle aggregates formed in a solution of 5 mM  $\text{C}_{10}\text{-C}_{15}$  fatty acids in 100 mM  
604 NaCl as observed by confocal microscopy (**a**) and NS-TEM (**b**, **c**, and **d**). During NS-TEM, vesicles burst  
605 under vacuum leading to collapsed structures as seen in these micrographs.

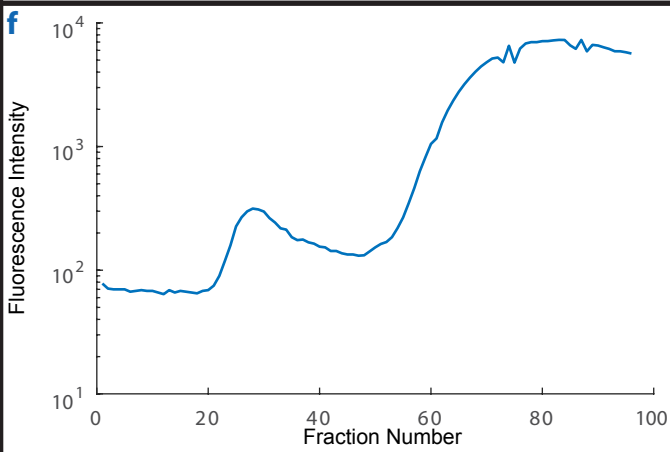
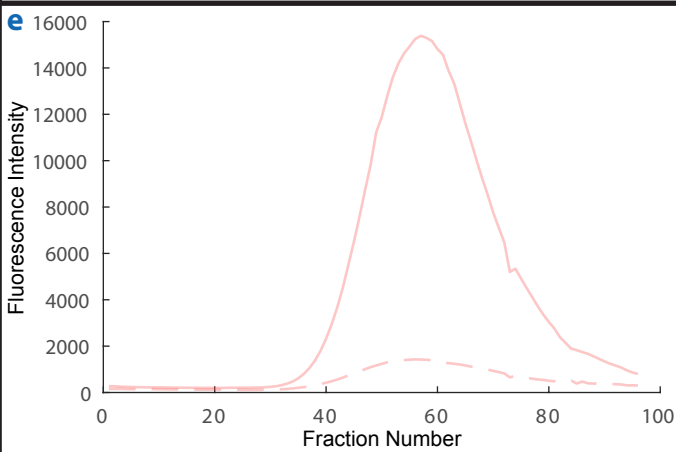
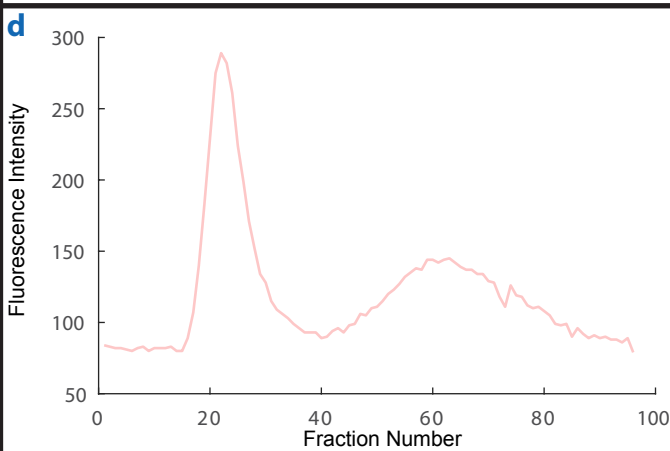
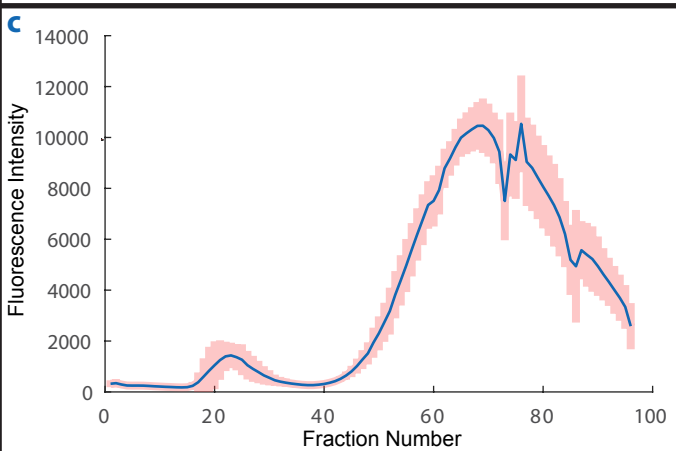
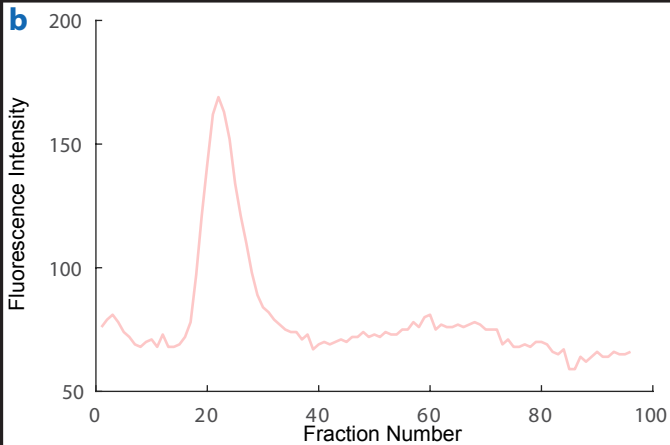
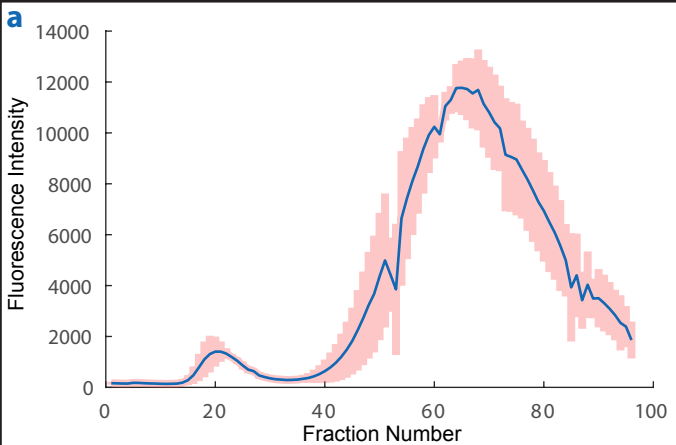
606

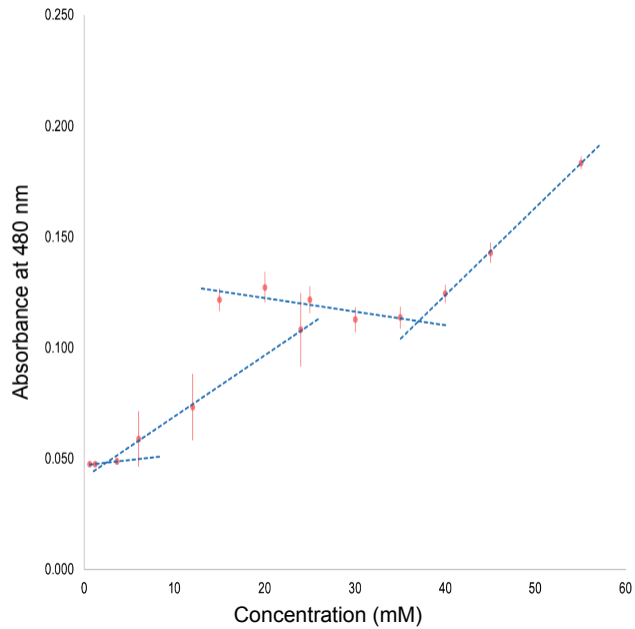
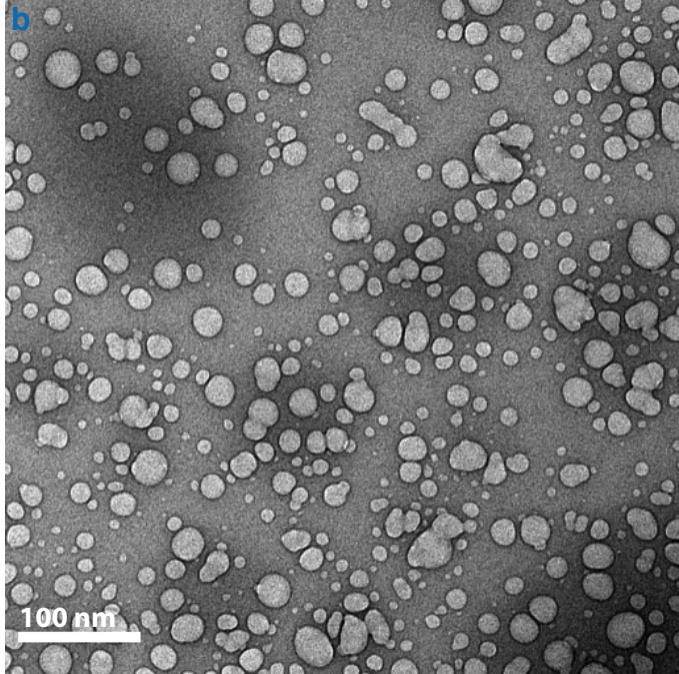
607 **Figure 7.** Confocal (**a**) and Cryo-TEM (**b**) micrographs of 5 mM 1:1:1  $\text{C}_{10}\text{-C}_{15}$  fatty acid/alcohol/ $\text{C}_{10}$   
608 isoprenoid mixture in a combined solution of 600 mM NaCl, 50 mM  $\text{MgCl}_2$ , and 10 mM  $\text{CaCl}_2$  at pH  
609 12.69 and 11.75 respectively.

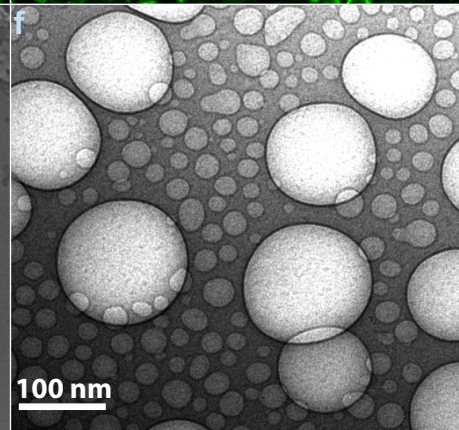
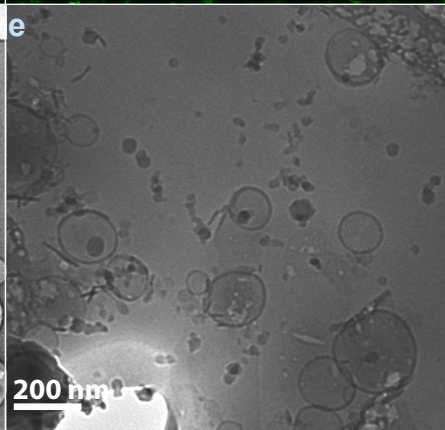
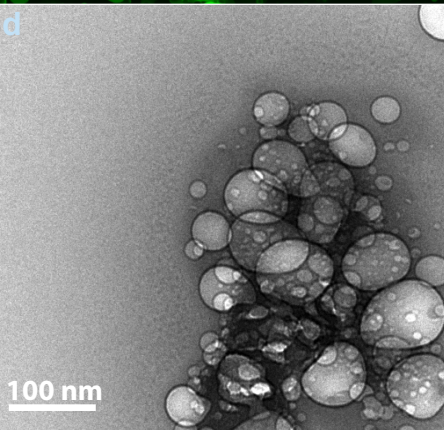
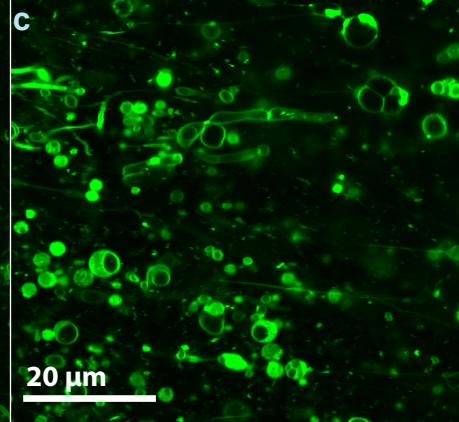
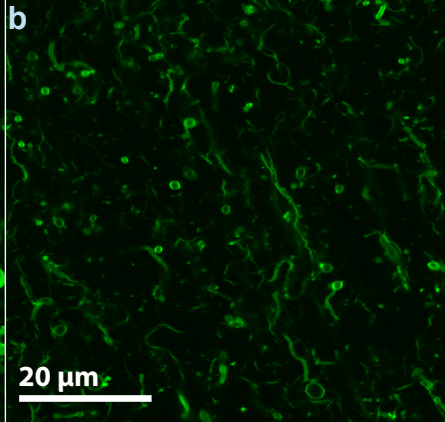
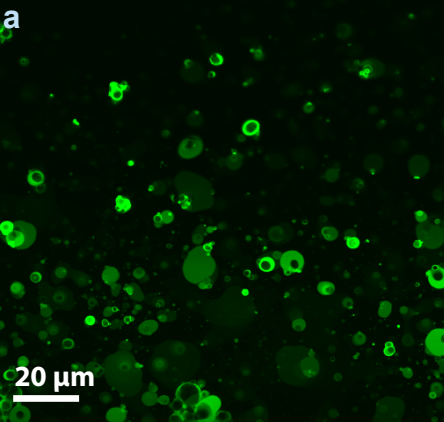
610

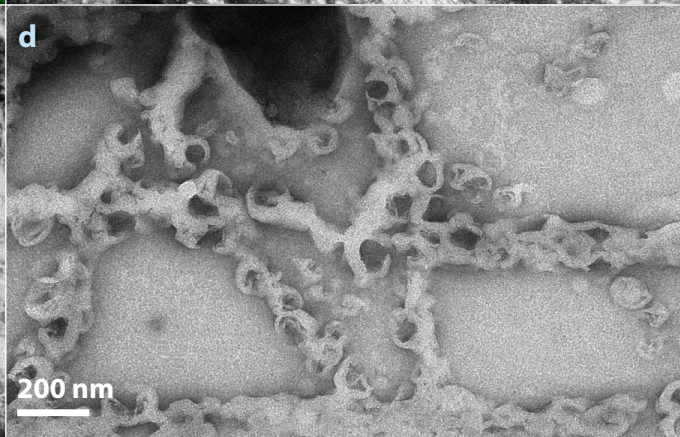
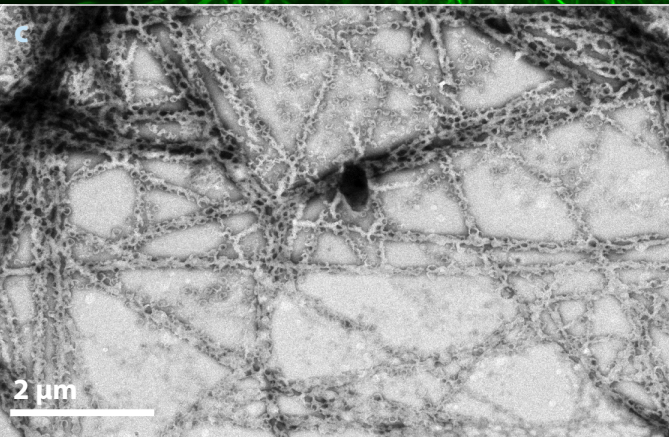
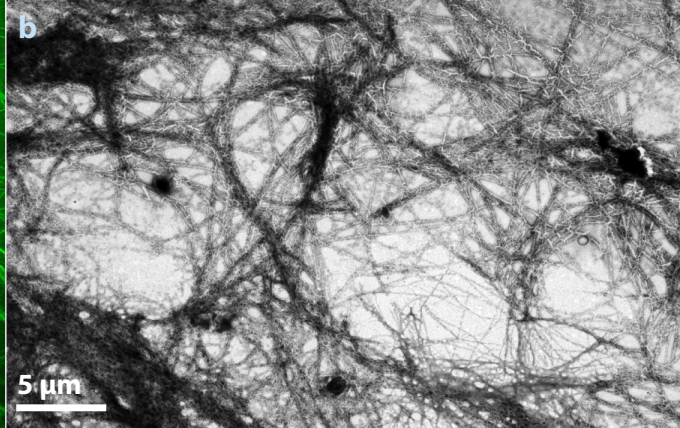
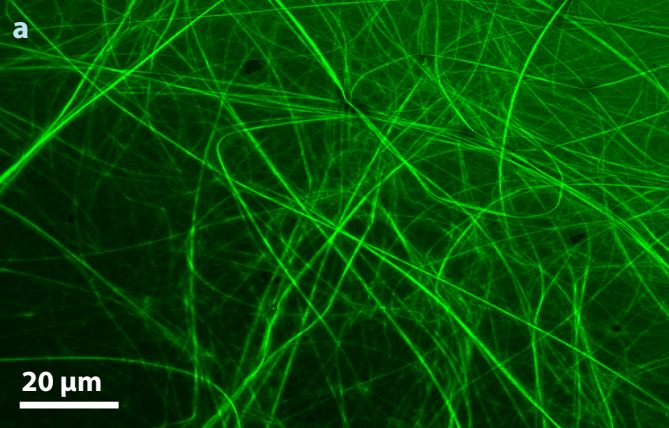




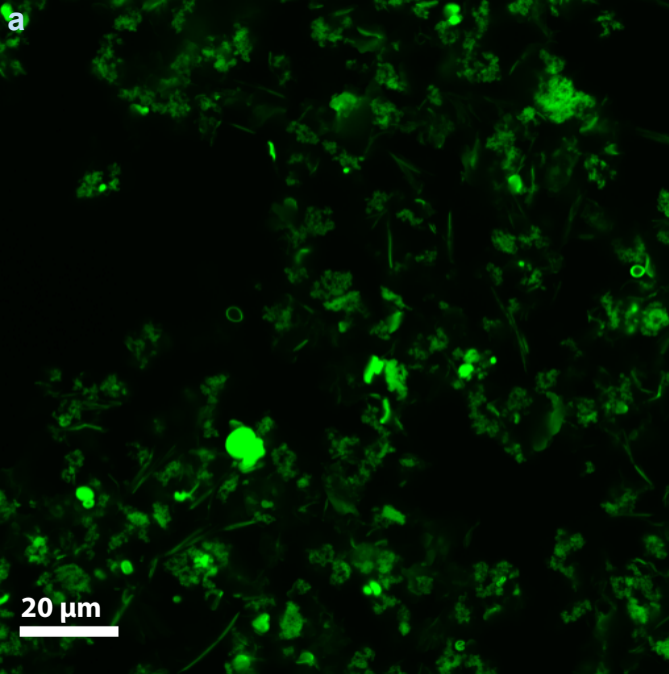
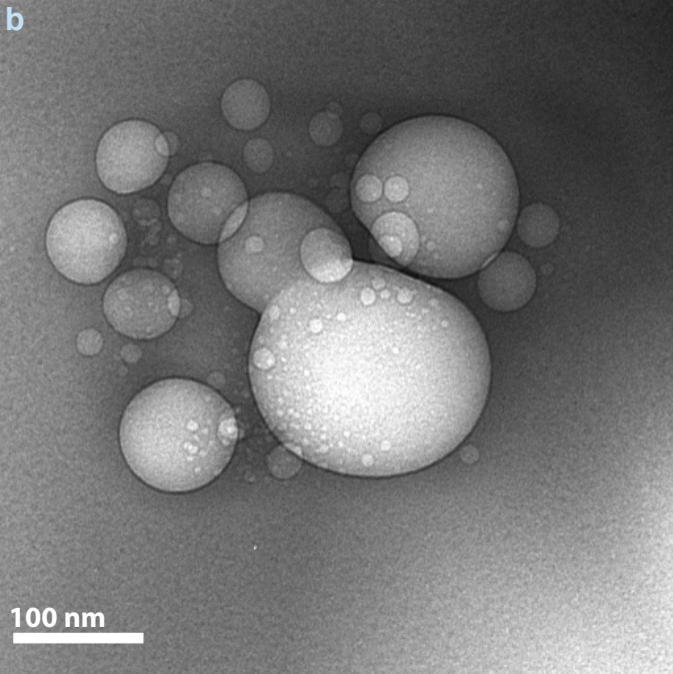


**a****b**







**a****b**

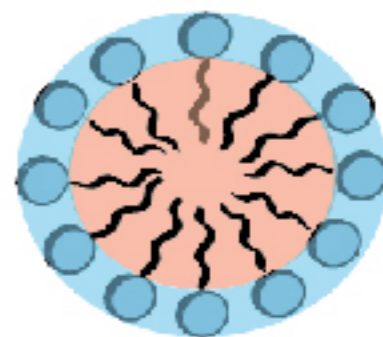
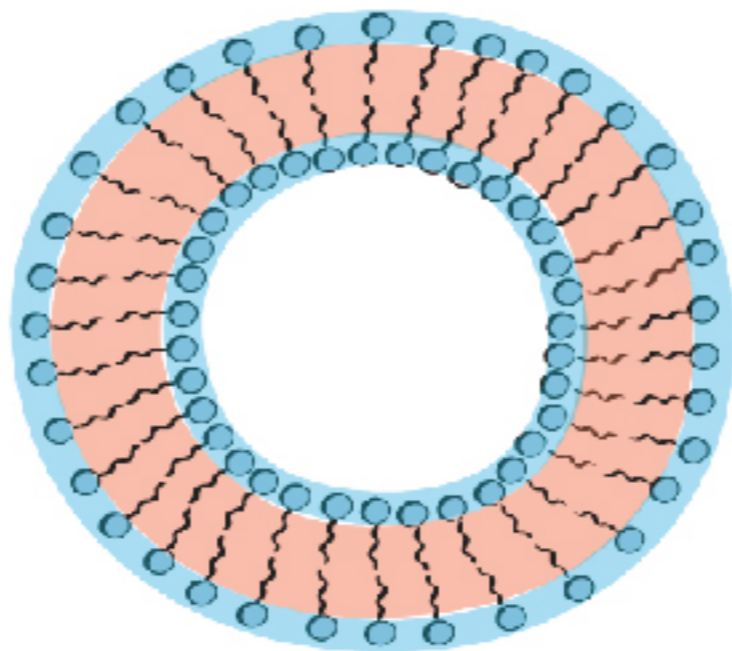
Droplet



Vesicle

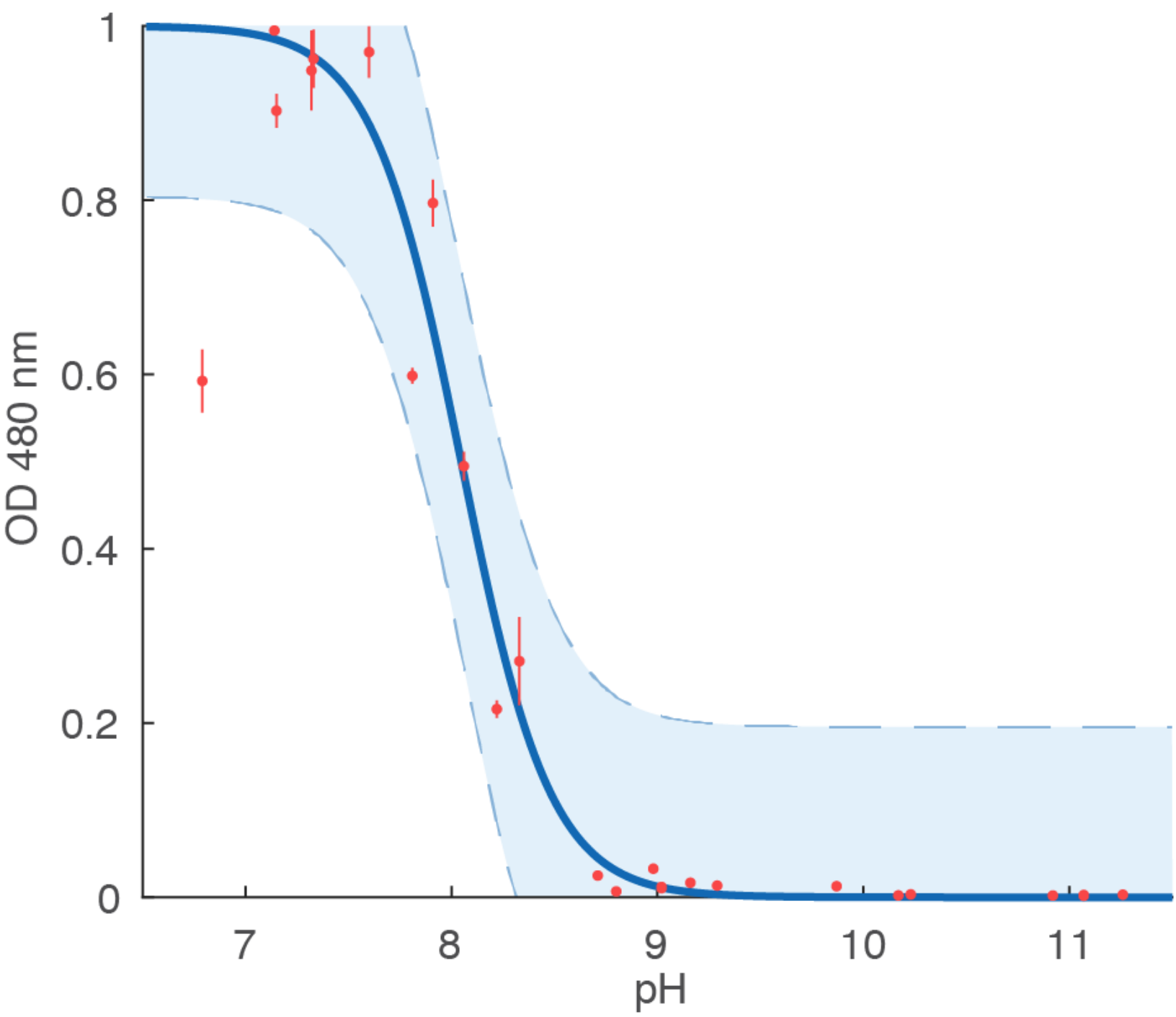


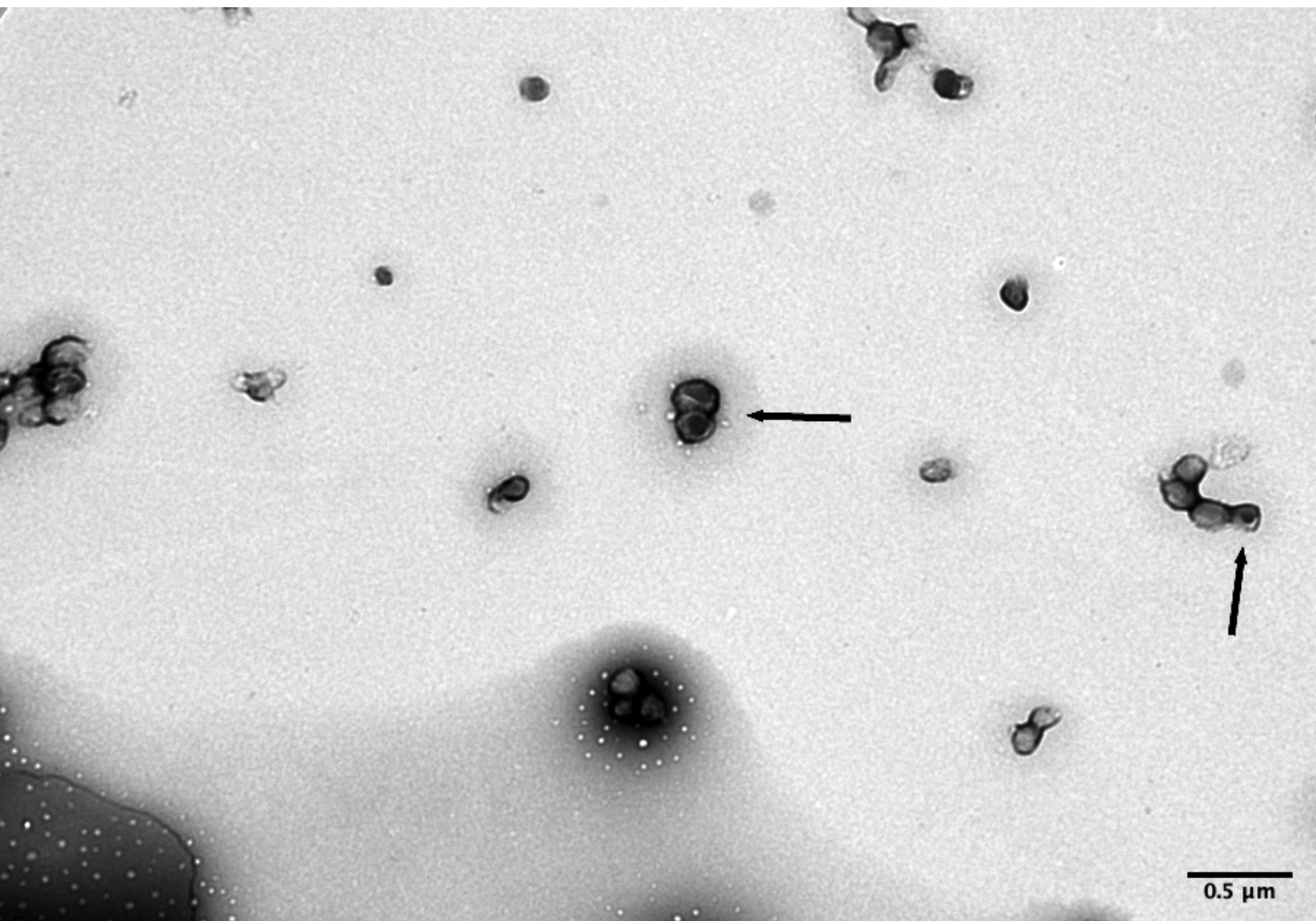
Micelle

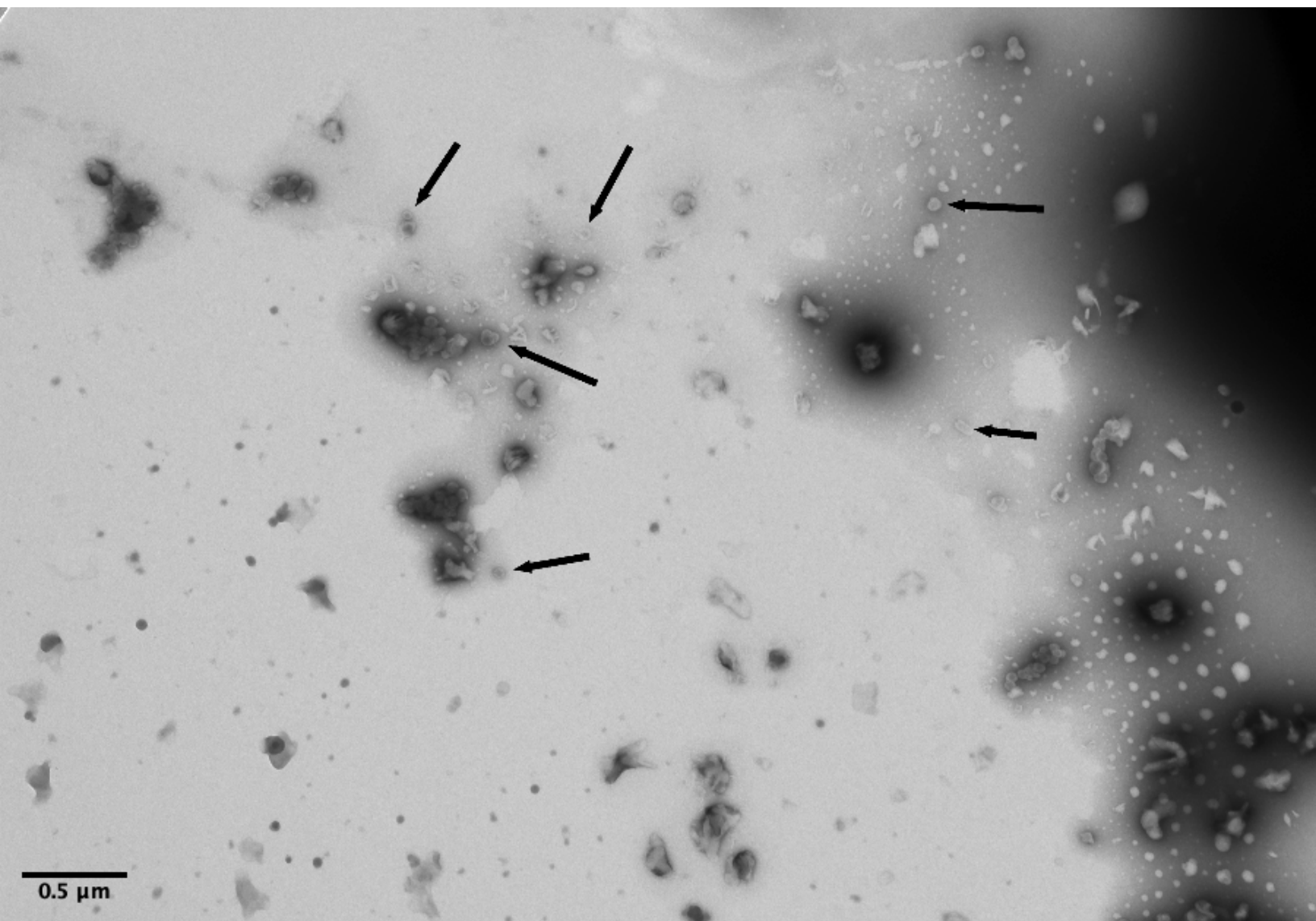


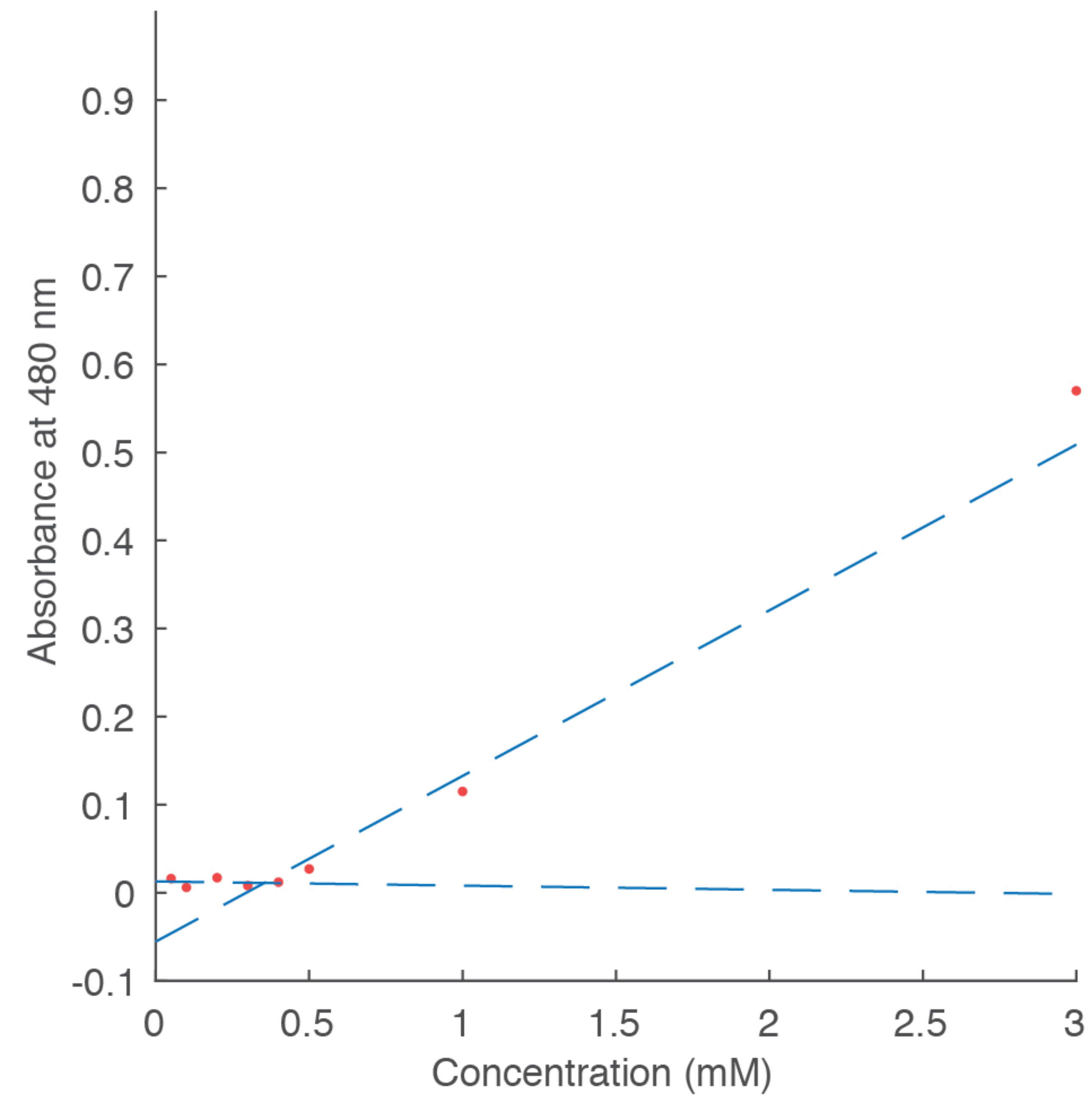
pH









**a****b**